International Journal of Pharmaceutics 644 (2023) 123344

Contents lists available at ScienceDirect

International Journal of Pharmaceutics

journal homepage: www.elsevier.com/locate/ijpharm

Evaluation of the therapeutic efficacy of ^{213}Bi-labelled DOTA-conjugated alpha-melanocyte stimulating hormone peptide analogues in melanocortin-1 receptor positive preclinical melanoma model

Csaba Csikos [a,b,1], Zita Képes [a,1], Anikó Fekete [a], Adrienn Vágner [c], Gábor Nagy [c], Barbara Gyuricza [a,d], Viktória Arató [a,e], Levente Kárpáti [f], István Mándity [f,g], Frank Bruchertseifer [h], Gábor Halmos [i], Dezső Szikra [a], György Trencsényi [a,b,*]

[a] Division of Nuclear Medicine and Translational Imaging, Department of Medical Imaging, Faculty of Medicine, University of Debrecen, Nagyerdei St. 98, H-4032 Debrecen, Hungary
[b] Gyula Petrányi Doctoral School of Clinical Immunology and Allergology, Faculty of Medicine, University of Debrecen, Nagyerdei St. 98, H-4032 Debrecen, Hungary
[c] Scanomed Ltd., Debrecen, Nagyerdei St. 98, H-4032 Debrecen, Hungary
[d] Doctoral School of Chemistry, Faculty of Science and Technology, University of Debrecen, Egyetem square 1, H-4032 Debrecen, Hungary
[e] Doctoral School of Pharmaceutical Sciences, University of Debrecen, Nagyerdei St. 98, H-4032 Debrecen, Hungary
[f] Department of Organic Chemistry, Faculty of Pharmacy, Semmelweis University, Hőgyes Endre St. 7, H-1092 Budapest, Hungary
[g] Artificial Transporters Research Group, Research Centre for Natural Sciences, Magyar tudósok Boulevard 2, H-1117 Budapest, Hungary
[h] European Commission, Joint Research Centre (JRC), Karlsruhe, Germany
[i] Department of Biopharmacy, Faculty of Pharmacy, University of Debrecen, Nagyerdei St. 98, H-4032 Debrecen, Hungary

ARTICLE INFO

Keywords:
Alpha-melanocyte stimulating hormone-analogue (α-MSH analogue)
Bismuth-213
[^{213}Bi]Bi-DOTA-HOLDamide
[^{213}Bi]Bi-DOTA-NAPamide
Melanocortin-1 receptor (MC1-R)
Melanoma malignum (MM)
Radionuclide therapy

ABSTRACT

Melanocortin-1 receptor (MC1-R) targeting alpha-melanocyte stimulating hormone-analogue (α-MSH) biomolecules labelled with α-emitting radiometal seem to be valuable in the targeted radionuclide therapy of MC1-R positive melanoma malignum (MM). Herein is reported the anti-tumor *in vivo* therapeutic evaluation of MC1-R-affine [^{213}Bi]Bi-DOTA-NAPamide and HOLDamide treatment in MC1-R positive B16-F10 melanoma tumor-bearing C57BL/6J mice. On the 6th, 8th and 10th days post tumor cell inoculation; the treated groups of mice were intravenously injected with approximately 5 MBq of both amide derivatives. Beyond body weight and tumor volume assessment, [^{68}Ga]Ga-DOTA-HOLDamide and NAPamide-based PET/MRI scans, and *ex vivo* biodistribution studies were executed 30,- and 90 min postinjection. In the PET/MRI imaging studies the B16-F10 tumors were clearly visualized with both ^{68}Ga-labelled tracers, however, significantly lower tumor-to-muscle (T/M) ratios were observed by using [^{68}Ga]Ga-DOTA-HOLDamide. After alpha-radiotherapy treatment the tumor size of the control group was larger relative to both treated cohorts, while the smallest tumor volumes were observed in the NAPamide-treated subclass on the 10th day. Relatively higher [^{213}Bi]Bi-DOTA-NAPamide accumulation in the B16-F10 tumors (%ID/g: 2.71 ± 0.15) with discrete background activity led to excellent T/M ratios, particularly 90 min postinjection. Overall, the therapeutic application of receptor selective [^{213}Bi]Bi-DOTA-NAPamide seems to be feasible in MC1-R positive MM management.

1. Introduction

Targeted radionuclide therapy (TRNT) has been demonstrated as an effective anti-tumor treatment. Application of cancer therapy with alpha emitter radionuclides displays excellent efficacy both at preclinical and clinical levels (Kratochwil et al., 2014; Norenberg et al., 2006; Poty et al., 2018; Sgouros et al., 2020).

High linear energy transfer (LET: ≈100 keV/μm) along with the short pathway of the alpha particles within the tissue (40–80 μm, approximately 2–10 cell diameter) make bismuth-213 (^{213}Bi; $t_{1/2}$ = 45.6 min)

* Corresponding author at: Division of Nuclear Medicine and Translational Imaging, Department of Medical Imaging, Faculty of Medicine, University of Debrecen, Nagyerdei St. 98, H-4032 Debrecen, Hungary.
E-mail address: trencsenyi.gyorgy@med.unideb.hu (G. Trencsényi).
[1] These authors contributed equally to this study.

https://doi.org/10.1016/j.ijpharm.2023.123344
Received 20 April 2023; Received in revised form 20 July 2023; Accepted 21 August 2023
Available online 25 August 2023
0378-5173/© 2023 The Authors. Published by Elsevier B.V. This is an open access article under the CC BY-NC-ND license (http://creativecommons.org/licenses/by-nc-nd/4.0/).

an exquisite candidate for targeted alpha therapy (TAT) (Ahenkorah et al., 2021; Dekempeneer et al., 2020; Morgenstern et al., 2018; Wild et al., 2011). These physical properties ensure irreversible, selective antitumor effect without untoward toxicity on intact tissues (Ahenkorah et al., 2021; Dekempeneer et al., 2016). Its easy accessibility from actinium-225/bismuth-213 (^{225}Ac/^{213}Bi) generator system purveys a clear added value for the radiometal (Morgenstern et al., 2012). Beyond therapeutic applications, due to the accompanying gamma (γ) radiation, ^{213}Bi is well-suited for diagnostics purposes, which makes the radiometal a promising theranostic agent (Ahenkorah et al., 2021; Castillo et al., 2022; Barca et al., 2021).

Experiments with radiotracers targeting receptors expressed in tumors represent a bridge between translational discoveries and their clinical integration both in diagnostic and therapeutic scenarios. Either α-melanocyte-stimulating hormone (α-MSH) analogue NAPamide (Ac-Nle-Asp-His-d-Phe-Arg-Trp-Gly-Lys-NH2) or its DOTA (1,4,7,10-tetraazacyclododecane-1,4,7,10-tetraacetic acid) conjugated (DOTA-NAPamide) derivative labelled with radioisotopes were confirmed as valuable molecular probes in the imaging of melanocortin-1 receptor (MC1-R) positive malignant melanoma (MM) (Brzoska et al., 2008; Nagy et al., 2017; von Hacht et al., 2019). Nagy *et al.* confirmed the diagnostic feasibility of scandium-44 (^{44}Sc)-labelled DOTA-NAPamide in B16-F10 melanoma cells and tumor-bearing C57BL/6J mice (Nagy et al., 2017). The tumor targeting ability of NAPamide linked to gallium-68 (^{68}Ga) or indium-111 (^{111}In) was also reported at preclinical level (Cheng et al., 2002; Froidevaux et al., 2004).

Beyond imaging purposes, radiolabelled molecules targeting MM, including MC1-R, would represent useful tools in current melanoma treatment. An earlier study confirmed the therapeutic adequacy of 9.2.27 melanoma antibody labelled with α-emitting ^{213}Bi-, and positron emitter terbium-152 (^{152}Tb) in the treatment of micrometastatic MM (Abbas et al., 2000). Investigating the *in vivo* anti-tumor efficacy of another ^{213}Bi-labelled melanoma monoclonal antibody (α-immunoconjugate/^{213}BiAIC) in melanoma xenografts of nude mice, revealed a noteworthy tumor growth inhibition and regression upon the intralesional administration of 12.5–200 microCi of ^{213}BiAIC (Allen et al., 2001). In addition, ^{225}Ac-DOTA-MC1-R ligand (^{225}Ac-DOTA-MC1RL) proved to be highly valuable in lengthening the lifespan and decelerating both the tumor and metastases formation of MC1-R positive human uveal melanoma tumor-bearing (MEL270) mice (Tafreshi et al., 2019).

As battling against MM and pertinent metastases represents one of the major challenges in todays' science, receptor-specific imaging radiopharmaceuticals with the replacement of the diagnostic radiometal with its therapeutic sister seem to be promising in personalized theranostic cancer treatment (Filippi et al., 2020; Gladfelter et al., 2017; Marin et al., 2020; Sadler et al., 2022). Considering the favourable physical characteristics of ^{213}Bi, it may be an ideal candidate for theranostic applications.

Our research group previously reported the radiolabelling methods, the ex vivo biodistribution, dosimetry and melanoma targeting potential of the newly synthesized ^{213}Bi-labelled DOTA-conjugated MC1-R-affine α-MSH analogues: NAPamide, and – HOLDamide (Kálmán-Szabó et al., 2023). Driven by these prior research findings, herein is reported the assessment of the therapeutic effectiveness of ^{213}Bi-labelled, MC1-R specific, α-MSH analogue NAP, - and HOLDamide in established MCR-1 positive B16-F10 tumor-bearing preclinical model systems. Prior to the treatment, positron emission tomography/magnetic resonance imaging (PET/MRI) applying [^{68}Ga]Ga-DOTA-NAPamide and [^{68}Ga]Ga-DOTA-HOLDamide was performed to verify the presence of the tumors.

2. Materials and methods

2.1. Peptide synthesis

We purchased DOTA-HOLDamide from Caslo (Kongens Lyngby, Denmark) in a form of resin-bound peptide (DOTA(tBu)$_3$-Gly-pY-OBzl-Nle-Asp(OtBu)-His(Trt)-(D-Phe)-Arg(Pbf)-Trp(Boc)-(Rink Amide MBHA resin, 1562 g/mol), while DOTA-NAPamide (NH_2-Lys(DOTA)-Gly-Trp-Arg-DPhe-His-Asp-Nle-Ac, Mw: 1485.7 g/mol) was synthetized in continuous flow.

The resin bound DOTA-HOLDamide was assembled by the utilization of Fmoc-amino acids with the utilization of DIC/HOBt coupling agents. The Fmoc deprotection was carried out *using* 20% piperidin solution.

The DOTA-NAPamide peptide was synthetized on solid support in continuous flow on a Tentagel R RAM resin (0.20 mmol g^{-1}) on a 0.03 mmol scale with 0.045 mmol Fmoc-protected amino acid and 0.045 mmol HATU as coupling reagent dissolved in 1 mL *N, N'*-dimethylformamide (DMF) (Mándity et al., 2014; Mándity et al., 2016). The coupling reactions were carried out at the reaction conditions as follows, 60 bar pressure, 70 °C temperature, 0.15 mL min^{-1} flow rate. For deprotection 1 mL of 2% DBU 2% piperidine PC solution has been used. Between two chemical steps DMF was used for washing for 5 min with 0.15 mL min^{-1} flow rate. The residence time at this flow rate was 5 min, with a 125*4 mm column dimension.

Peptides were cleaved from the resin with the cleavage cocktail as follows: trifluoroacetic/water/DL-dithiothreitol/triisopropylsilane (90:5:2.5:2.5). The purification was carried out by RP-HPLC, using a Phenomenex Luna C18 100 Å 10 μm column (10 mm × 250 mm). The HPLC apparatus was made by JASCO. The solvent system used was as follows: eluent A − 0.1% TFA in water; eluent B − 0.1% TFA in 80% acetonitrile in water; a linear gradient was used for 60 min starting form 20% B finished at 50% B, at a flow rate of 4.0 mL min^{-1}, with detection at 206 nm. The purities of the fractions were determined by analytical RP-HPLC using a JASCO HPLC system with a Phenomenex Luna C18 100 Å 5 μm column (4.6 mm × 250 mm) and the pure fractions were pooled and lyophilized. The purified peptides were characterized by mass spectrometer (MS), using a Bruker HCT II ETD MS equipped with an Agilent 1200 HPLC system.

The purified peptides were used for labelling chemistry. The scheme of the peptide synthesis is presented in Supplementary Material **Fig. S1**. DOTA-NAPamide and DOTA-HOLDamide were identified on a BEH C18 1.7 μm 2.1 × 50 mm column using Waters Acquity I-Class UPLC liquid chromatography system with PDA detector coupled to a Xevo G2 QT of MS. The results of the mass spectrometry can be seen in Supplementary Material **Fig. S2.**

2.2. Radiochemistry

2.2.1. Synthesis of [^{68}Ga]Ga-DOTA-NAPamide and [^{68}Ga]Ga-DOTA-HOLDamide

Five mL 0.05 M ultra-pure HCl was used for the elution of the Germanium-68/Gallium-68 (^{68}Ge/^{68}Ga) generator. Incubation of a mixture of ^{68}Ga-solution (375 μL, 80–130 MBq), NH_4OAc buffer (120 μL, 0.5 M, pH = 4) and stock solution of DOTA-NAPamide and DOTA-HOLDamide (5 μL, 1 mg/mL, 0.673 M) was carried out for 15 min at 95 °C. Following the transport of the solution to the Strata-X cartridge containing 1 mL 96% EtOH, 5 mL H_2O and 1 mL 0.25 M pH = 4 NH_4OAc, the buffer was removed with 1 mL H_2O. Then, the solution was eluated using EtOH (300 μL 96%). Followed by evaporation under N_2 flow at 95 °C, the dry product was taken up utilizing PBS (200 μL). Waters Acquity BEH C18 column (1.7 μm, 3 × 50 mm) was applied for the radio-HPLC-based measurement of the radiochemical purity (RCP) of the product. Fig. 1. represents the chemical structure of the labelled compounds.

2.2.2. Synthesis [^{213}Bi]Bi-DOTA-NAPamide and [^{213}Bi]Bi-DOTA-HOLDamide

As we described earlier in our previous study, ^{213}Bi was eluted from an Actinum-225/Bismuth-213 (^{225}Ac/^{213}Bi) generator (Kálmán-Szabó et al., 2023). Stock solutions (1 mg/mL) were produced from the DOTA-conjugated amide derivatives. DOTA-NAPamide and DOTA-HOLDamide

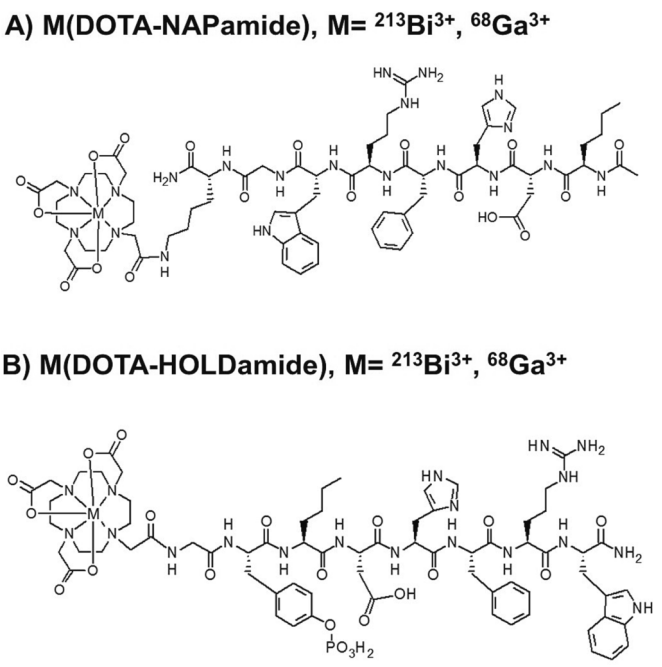

Fig. 1. The chemical structure of the radiolabelled peptides.

solutions of 5 μL (3.4 and 3.2, nmol peptide; respectively) were mixed with 600 μL ^{213}Bi corresponding to 95 ± 20 MBq, 135 μL 2 M TRIS buffer (0.34 M) and 50 μL 20% ascorbic acid (72 mM) at pH level of 8.7. The mixture of 20 μL of ^{213}Bi, 30–35 μmol sodium citrate and the stock solutions of the DOTA-conjugated peptides (approximately 10 nmol DOTA-NAPamide or DOTA-HOLDamide) was used for *LogP* measurements and serum stability determination. Following the incubation (5 min at 95 °C) and cooling, the mixture was transferred to Solid Phase Extraction (SPE) cartridge (Oasis HLB 1 cc (30 mg) Extraction Cartridge; Waters). After dropwise elution and evaporation, the labelled product was dissolved in PBS. Instant Thin Layer Chromatography impregnated with silica gel (iTLC-SG; Varian) was used for the identification of RCP by radio-TLC (Kálmán-Szabó et al., 2023). The chemical structure of the labelled amide derivatives is presented in Fig. 1.

2.3. LogP measurements

A mixture containing 10 μL of approximately 5 MBq of [^{68}Ga]Ga-DOTA-NAPamide or [^{68}Ga]Ga-DOTA-HOLDamide solution, 500 μL of 1-octanol and 490 μL of water was shaken (600 rpm) and centrifugated (6000 rpm) for 10 and 5 min; respectively. The supernatant was collected and diluted with water from both samples. Gamma counter was applied for the determination of the radioactivity of the fractions. The measurements were accomplished three times in case of both the NAPamide and the HOLDamide derivatives. In case of the ^{213}Bi-conjugated peptides, the mixture of 10 μL of the ^{213}Bi-conjugated DOTA-NAPamide aqueous peptide in PBS solution, 0.49 mL water and 0.5 mL 1-octanol was shaken for 20–30 min, and post centrifugation, samples of 100 μL were taken from each layer for radioactivity determination performed with a calibrated gamma counter (Perkin-Elmer Packard Cobra, Waltham, MA, USA) (Kálmán-Szabó et al., 2023).

2.4. Serum stability measurements

To determine serum stability 10 μL of [^{68}Ga]Ga-DOTA-NAPamide or [^{68}Ga]Ga-DOTA-HOLDamide or ^{213}Bi-conjugated NAPamide or ^{213}Bi-conjugated HOLDamide solution was mixed with the solution of 90 μL of mouse plasma, Na_2EDTA (0.01 M) and oxalic acid (0.01 M). Radio-HPLC was applied to analyse the samples at the starting point and 30, − 60, - and 120 min thereafter.

2.5. Cell culturing

B16-F10 cells (mouse melanoma, RCB Cat# RCB2630, RRID: CVCL_0159) were purchased from American Type Culture Collection (CRL-6475™, ATCC, Virginia, USA). Cell culturing was accomplished in GlutaMAX™ Dulbecco's Modified Eagle's Medium (DMEM) (Gibco™, Beijing, China) supplemented with antimycotic (1% (vol/vol); Gibco™), and antibiotic solution (1% (vol/vol); Gibco™) as well as heat-inactivated fetal bovine serum (FBS, 10% (vol/vol); Gibco™). Minimum Essential Medium (MEM) non-essential amino acid solution (1% (vol/vol); Gibco™) and MEM vitamin solution (1% (vol/vol); Gibco™) were added to the medium of the B16-F10 cell culture. With the application of T75 flasks (Sarstedt Ltd., Budapest, Hungary) tumor cells were cultured in cell culture incubator ESCO CCL-170B-8 (37 °C, 5% CO_2, 95% humidity). Tumor cell inoculation occurred following five passages. Trypan blue exclusion test was applied for cell viability verification.

2.6. Animal housing

Twelve-week-old C57BL/6J mice (n = 50) were purchased from Charles River Laboratories (Animalab Ltd., Budapest, Hungary). The experimental small animals were kept under standard conditions in Individually Ventilated Cages (IVC) with regulated ambient temperature of 24 ± 2 °C and at relative humidity of 55 ± 10%. Conventional circadian 12-hour light/dark cycle (7:00p.m. to 7:00 a.m.) was ensured. All animals were provided *ad libitum* with sterile semi-synthetic diet (Akronom Ltd., Budapest, Hungary) and sterile drinking water. All procedures complied with all applicable sections of the Hungarian Laws and the directions and regulations of the European Union and had the permission of the Ethics Committee for Animal Experimentation of the University of Debrecen (ethical permission number: 16/2020/DEMÁB). All efforts were made to fulfil the requirements of 3R policy.

2.7. B16-F10 tumor generation

A dedicated small animal anaesthesia device (Tec3 Isoflurane Vaporizer, Eickemeyer Veterinary Equipment, Luton, UK) utilizing 3% isoflurane (Forane, AbbVie, Chicago, IL, USA), 0.4 L/min O_2, and 1.4 L/min N_2O was employed to anaesthetize the mice to generate the experimental tumors. $2x10^6$/100 μL B16-F10 (mouse melanoma) cells in 120 μL of sterile saline were injected subcutaneously *(s.c.)* into the shaved left shoulder area of the C57BL/6J mice. The tumor size was calculated using the following formula: (largest diameter × smallest diameter^2)/2. Calliper measurements were used for the assessment of tumor growth. *In vivo* PET/MRI imaging and *ex vivo* experiments were conducted 10 ± 1 days post tumor cell transplantation at a tumor volume of approximately 200 ± 10 mm^3. We used cells after similar passage numbers for the tumor induction of the small animals involved in both imaging and therapeutic studies.

The subsequent criteria were used for mice euthanization: tumor burden greater or equal to 10% of the animal's normal body weight, tumor exceeding 1.5 cm in size in any directions, diminishing scores of animal's body condition, tumor preventing ambulation or ability to reach food or water, severely ulcerated or abscessed tumor, or a tumor causing significant pain and distress.

2.8. Cancer treatment studies

Six days after the tumor cell implantation the B16-F10 tumor-bearing mice – with an average tumor volume of 5 mm^3 - were randomly categorized into three different subgroups: untreated (control, n = 5), [^{213}Bi]Bi-DOTA-NAPamide (n = 9) treated and [^{213}Bi]Bi-DOTA-HOLDamide (n = 6) treated groups. On the 6th, 8th and 10th days post tumor

cell inoculation, the experimental mice of the NAPamide and HOLDamide treated subcategories were intravenously *(i.v.)* treated with approximately 5, - and 5 MBq of [^{213}Bi]Bi-DOTA-NAPamide (0.43 ± 0.17 nmol/injection) and [^{213}Bi]Bi-DOTA-HOLDamide (0.34 ± 0.10 nmol/injection); respectively. The control animals were *i.v.* injected with 150 μL saline solution.

2.9. In vivo small animal PET/MRI imaging

To verify the presence of the B16-F10 tumors *in vivo* static small animal PET/MRI examinations were conducted 10 ± 1 days following the tumor cell inoculation. Scans were acquired on nanoScan PET/MRI (Mediso Ltd., Budapest, Hungary). Sixty minutes after the intravenous *(i.v.)* injection of the mice with approximately 10 MBq [^{68}Ga]Ga-DOTA-HOLDamide (approximately 2.3 nmol/ injection) or [^{68}Ga]Ga-DOTA-NAPamide (approximately 0.5 nmol/injection); we subjected the experimental animals to static T1 PET/MRI acquisition (20 min acquisition time/bed position) applying a preclinical PET/MRI system (nanoScan PET/MRI 1 T, Mediso Ltd., Budapest, Hungary). Isoflurane (AbbVie, Budapest, Hungary; OGYI-T-1414/01) induced anaesthesia was executed with a dedicated small animal anaesthesia device (Tec3 Isoflurane Vaporizer, Eickemeyer Veterinary Equipment, Luton, UK) during the whole examination. Following a 3D ordered-subsets-expectation–maximization line-of-response (OSEM-LOR) image reconstruction, with the help of the BrainCAD image analysis software, volume of interests (VOIs) were manually placed around the tumor and the following examined organs and tissues: brain, lung, stomach, kidney, heart, liver, intestines, fat tissue, and muscle. As part of PET data analysis standardized uptake values (SUV) including SUV_{mean} and SUV_{max} were registered. SUV (g/mL) referring to the radiopharmaceutical concentration within the VOI is calculated with the help of the injected dose and the weight of the animal as follows:

SUV = [VOI activity (Bq/mL)]/[injected activity (Bq)/animal-weight (g)].

SUV_{mean} and SUV_{max} indicate the average activity concentration of the VOI and the voxel with the most elevated tracer activity within the VOI; respectively. Tumor-to-background/muscle (T/M) ratios were also determined based on the radioactivity of the tumor and the background muscle.

2.10. Ex vivo organ distribution studies

With the application of 5% Forane the treated B16-F10 tumor-bearing mice were euthanized 30, - and 90 min postinjection of [^{213}Bi]Bi-DOTA-HOLDamide and [^{213}Bi]Bi-DOTA-NAPamide. For euthanasia we applied the currently valid general guidelines for rodents in experimental tumor studies. Following dissection and weight measurements, the radioactivity of the tumors and various organs and tissues was determined with a calibrated gamma counter (Hewlett Packard Cobra II Autogama Gamma Counter, Waltham, MA, USA). The accumulation of [^{213}Bi]Bi-DOTA-HOLDamide and [^{213}Bi]Bi-DOTA-NAPamide was presented as the mean values of the percent administered dose per gram (% ID/g) tissue.

2.11. Statistical analyses

For the accomplishment of statistical analyses MedCalc 18.5 commercial software package (MedCalc 18.5, MedCalc Software, Mariakerke, Belgium) was utilized. Student's *t*-test (two-tailed), two-way ANOVA, and Mann-Whitney *U* test were applied to determine the level of significance. Figures are demonstrated as mean ± SD of at least three independent experiments. Changes with $p < 0.05$ were considered to be significant, unless otherwise indicated.

3. Results and discussion

3.1. Chemistry

3.1.1. Characterization of [^{68}Ga]Ga-DOTA-NAPamide and [^{68}Ga]Ga-DOTA-HOLDamide

Specific activity was attained in case of both [^{68}Ga]Ga-DOTA-NAPamide (19–23 GBq/μmol) and [^{68}Ga]Ga-DOTA-HOLDamide (4.34 GBq/μmol). Regarding the ^{68}Ga-labelled NAPamide molecule, RCP exceeding 99% was registered, while as for the ^{68}Ga-labelled HOLDamide compound 86% and 99% were detected after the labelling reaction and the SPE purification; respectively. These results support successful radiolabelling that makes examinations at cellular and tissue level as well as *in vivo* possible. The decay corrected radiochemical yield (RCY) was detected to be between 80 and 86% for the ^{68}Ga-labelled NAPamide compound, whereas it was 65% for [^{68}Ga]Ga-DOTA-HOLDamide. The retention time measured in case of [^{68}Ga]Ga-DOTA-NAPamide and [^{68}Ga]Ga-DOTA-HOLDamide were 1.829 and 1.825 min; respectively with the HPLC method (as seen in Supplementary Material **Fig. S3.**).

The octanol/water partition coefficients were −3.50 and −2.5 for [^{68}Ga]Ga-DOTA-NAPamide, and for [^{68}Ga]Ga-DOTA-HOLDamide; respectively. Based on the hydrophilic nature of the tracers, elimination occurs via the kidneys. The stability determination showed that [^{68}Ga]Ga-DOTA-NAPamide suffered a 6.0%, a 2.5% and a 0.8% ^{68}Ga loss in the mouse plasma, in Na_2EDTA and in oxalic acid solution. These stability measurements verify that both assessed probes remain stable when used *in vivo*. The detailed radiochemical data are summarized in Supplementary Material **Table S1**.

3.1.2. Characterization of [^{213}Bi]Bi-DOTA-NAPamide and [^{213}Bi]Bi-DOTA-HOLDamide

[^{213}Bi]Bi-DOTA-NAPamide and [^{213}Bi]Bi-DOTA-HOLDamide were produced with high specific activity (13 GBq/μmol for the NAPamide and the HOLDamide derivative). The RCP was always higher than 99% in case of both radiotracers. Therefore, we managed to attain the effective radiolabelling of both amide derivatives with RCP over 99% and with a remarkable specific activity. This is highly satisfactory for the accomplishment of both *in vitro* and *in vivo* investigations. The decay corrected RCY was 70 ± 16% for [^{213}Bi]Bi-DOTA-NAPamide and 62 ± 7% for [^{213}Bi]Bi-DOTA-HOLDamide. TLC measurements showed that the ^{213}Bi-labelled peptides remain at start point (R_f = 0.0), while uncomplexed ^{213}Bi moves with the eluent (R_f = 0.6–0.7) (as presented in Supplementary Material **Fig. S4.**).

Based on stability investigations [^{213}Bi]Bi-DOTA-NAPamide and [^{213}Bi]Bi-DOTA-HOLDamide suffered ^{213}Bi loss to an extent of 3.5% and 1.4%; respectively. Serum stability measurements confirm that the investigated compounds remain stable during *in vivo* application. The *LogP* values for [^{213}Bi]Bi-DOTA-NAPamide and [^{213}Bi]Bi-DOTA-HOLDamide were −3.15 and −2.19; respectively. These results indicate the hydrophilic character of both imaging probes. Moreover, the ^{213}Bi-labelled NAPamide derivative was detected to be more hydrophilic in comparison with the ^{213}Bi-appended HOLDamide molecule. These observations were in line with our previous results, where the *LogP* values of the cyclotron produced $^{205/206}$Bi-conjugated DOTA-NAPamide and DOTA-HOLDamide were investigated (Kálmán-Szabó et al., 2023). According to the *LogP* results we suppose urinary way of excretion. **Table S2.** in the Supplementary Material displays the radiochemical data of the ^{213}Bi-labelled compounds.

3.2. In vivo PET/MRI imaging of B16-F10 tumor-bearing mice

In vivo whole-body PET/MRI examinations were executed for the verification of the presence of the *s.c.* growing B16-F10 tumors and for the assessment of the organ distribution of the MC1-R selective ^{68}Ga-labelled PET probes 60 min postinjection of 10 MBq [^{68}Ga]Ga-DOTA-HOLDamide and [^{68}Ga]Ga-DOTA-NAPamide into B16-F10 melanoma

tumor-bearing mice. We opted for *i.v.* administration in case of [^{68}Ga]Ga-DOTA-HOLDamide and [^{68}Ga]Ga-DOTA-NAPamide to obtain high quality images with better contrast. *In vivo* decay-corrected transaxial and whole-body coronal PET/MRI images of representative experimental mice are presented in Fig. 2**A and 2C**, and Fig. 2**B and 2D**; respectively.

Upon qualitative image evaluation the urinary system, including the kidneys and the urinary bladder were well detectable with both tracers; however, the radiopharmaceutical uptake was visually more prominent in case of [^{68}Ga]Ga-DOTA-HOLDamide relative to [^{68}Ga]Ga-DOTA-NAPamide. Based on the hydrophilic character of both radioisotopes - also confirmed by the LogP values - urinary excretion could be noted. Investigating the tumor-homing capability of [^{68}Ga]Ga-DOTA-NAPamide and [^{44}Sc]Sc-DOTA-NAPamide in MC1-R expressing B16-F10 tumor-bearing C57BL/6J mice, Nagy *et al.* also reinforced the renal route of elimination in case of both labelled probes (Nagy et al., 2017). According to the octanol–water partition coefficient, ^{111}In, - and ^{67}Ga-linked, DOTA-conjugated NAPamide (^{111}In-DOTA-NAP-amide, ^{67}Ga-DOTA-NAPamide) are also eliminated by the kidneys (Cheng et al., 2007a; Cheng et al., 2007b; Froidevaux et al., 2005). Further - *corresponding to the prior findings of Nagy and co-workers* – we registered moderate radiopharmaceutical uptake in other investigated abdominal and thoracic organs and tissues applying both the NAPamide and the HOLDamide derivatives (Nagy et al., 2017). In a like manner, negligible abdominal and thoracic tracer accumulation was depicted in the previous research of Cheng *et al.*, and Froidevaux *et al.* with ^{111}In-DOTA-NAPamide and ^{67}Ga-DOTA-NAPamide (Cheng et al., 2007a; Cheng et al., 2007b; Froidevaux et al., 2005). Albeit, in former studies dealing with fluorine-18 (^{18}F), - and copper-64 (^{64}Cu)-appended NAPamide derivatives increased radiotracer concentration and related poor T/M ratios were pinpointed in the lungs, stomach, liver, and the intestines (Cheng et al., 2007a; Cheng et al., 2007b). As satisfactory T/M ratios and high-quality image contrast are of critical importance regarding the correct interpretation of the PET scans, radiolabelling with ^{68}Ga seems to be superior to ^{18}F or ^{64}Cu labelling from clinical point of view. As presented in Fig. 2**A-2D** (yellow arrows) *s.c.* developing MC1-R over-expressing B16-F10 tumors could be definitely identified with both labelled α-MSH analogues 60 min after tracer application.

The quantitative comparative analyses of the *in vivo* figures of the selected organs and tissues did not reveal any considerable differences between the SUV_{mean} values of the ^{68}Ga-labelled NAPamide and HOL-Damide compounds ($p \leq 0.05$; demonstrated in Fig. 2**E-2G** and Supplementary Material **Table S3.**). Sixty minutes post administration of 10 MBq [^{68}Ga]Ga-DOTA-NAPamide slight radiopharmaceutical uptake was found in the brain, muscle, lung, stomach, heart, liver, fat tissue and the intestines with the following SUV_{mean} values: 0.02 ± 0.007, 0.03 ± 0.006, 0.06 ± 0.007, 0.07 ± 0,01, 0.1 ± 0.007, 0.12 ± 0.01, 0.05 ± 0.01, 0.07 ± 0.01; respectively. Identically, the brain (SUV_{mean}: 0.02 ± 0.007), the muscle (SUV_{mean}: 0.04 ± 0.006), the lung (SUV_{mean}: 0.06 ± 0.005), the stomach (SUV_{mean}: 0.07 ± 0.01), the heart (SUV_{mean}: 0.1 ± 0.01), the liver (SUV_{mean}: 0.12 ± 0.01), the adipose tissue (SUV_{mean}: 0.06 ± 0.03) and the intestines (SUV_{mean}: 0.1 ± 0.01) showed moderate

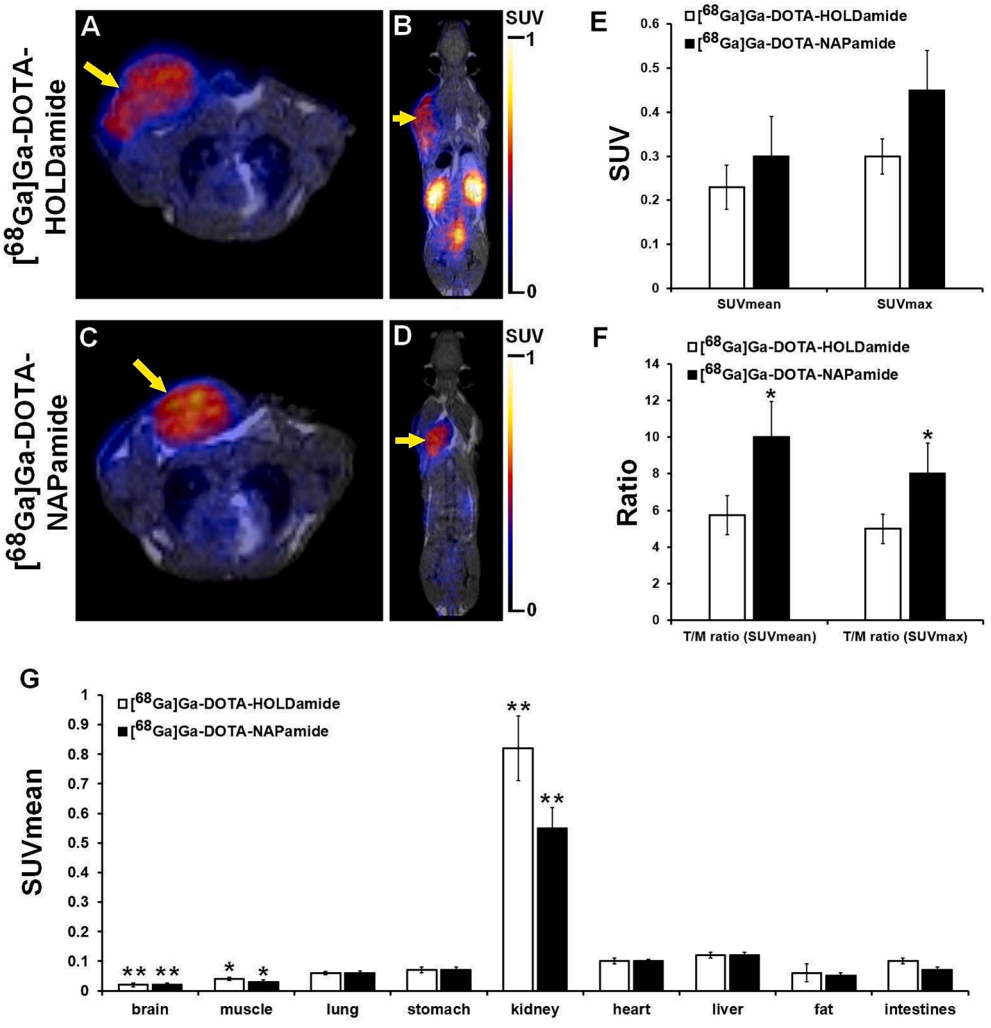

Fig. 2. *In vivo* PET/MRI imaging and quantitative image analysis of B16-F10 melanoma tumors using [^{68}Ga]Ga-DOTA-HOLDamide and [^{68}Ga]Ga-DOTA-NAPamide radiotracers. Representative decay-corrected transaxial (A, C) and whole-body coronal (B, D) PET/MRI images of MC1-R positive B16-F10 melanoma tumor-bearing C57BL/6J mice. Quantitative SUV analysis of [^{68}Ga]Ga-DOTA-HOLDamide and [^{68}Ga]Ga-DOTA-NAPamide accumulation in experimental B16-F10 melanoma tumors (E, F) and biodistribution results (G). n = 5 mice/radiopharmaceutical. Decay-corrected PET/MRI images and data were obtained 10 ± 1 days after subcutaneous tumor cell inoculation and 60 min after the intravenous injection of the radiotracers. Significance level between [^{68}Ga]Ga-DOTA-HOLDamide and [^{68}Ga]Ga-DOTA-NAPamide accumulation in B16-F10 tumors (F) and between the investigated organs (G): $p \leq 0.05$ (*), $p \leq 0.01$ (**). Yellow arrows: B16-F10 tumors. PET/MRI: positron emission tomography/magnetic resonance imaging; MC1-R: Melanocortin-1 Receptor; SUV: standardized uptake value; T/M: tumor-to-muscle ratio. (For interpretation of the references to colour in this figure legend, the reader is referred to the web version of this article.)

tracer accumulation in case of the radio-conjugated HOLDamide compound an hour after the injection. This is in line with the findings of Nagy *et al.*, who also encountered insignificant tracer accumulation with both the ^{68}Ga and the ^{44}Sc-labelled NAPamide derivatives in the abdominal and thoracic organs and tissues (Nagy et al., 2017). On the whole, the brain and the muscle demonstrated the least radioactivity with both imaging probes ($p \leq 0.05$ and $p \leq 0.01$ for the brain and the muscle; respectively). The slight cerebral uptake could be primarily explained by the physiological barrier function of the blood–brain barrier that possibly prohibits the entrance of these probes into the brain. Similarly, permeability-related factors may delineate such a reduced muscle accumulation.

In contrast, - *compared to the other organs* - notably marked SUV_{mean} figures were recorded in the kidneys applying both radiotracers ($p \leq 0.01$; [^{68}Ga]Ga-DOTA-NAP-amide and [^{68}Ga]Ga-DOTA-HOLDamide: 0.55 ± 0.07, and 0.82 ± 0.11; respectively). An hour after the administration of [^{68}Ga]Ga-DOTA-NAPamide, the SUV_{mean}, SUV_{max}, T/M SUV_{mean} and T/M SUV_{max} values of the B16-F10 tumors were 0.3 ± 0.09, 0.45 ± 0.09, 10 ± 1.94, 8 ± 1.69; respectively, whereas we registered the subsequent quantitative data regarding [^{68}Ga]Ga-DOTA-HOLDamide: SUV_{mean}: 0.23 ± 0.5, SUV_{max}: 0.3 ± 0.04, T/M SUV_{mean}: 5.75 ± 1.06 and T/M $SUV_{max.}$: 5.00 ± 0.80. Of note, relatively lower T/M values were encountered when applying the ^{68}Ga-labelled HOLDamide compound compared to the ^{68}Ga-labelled NAPamide agent which appeared to be statistically significant ($p > 0.05$). We suppose that the chemical properties and the stability of the labelled peptides may underpin the experienced disparity regarding the T/M ratios; however, future unbiased studies are required to fully uncover this issue (Breeman et al., 2011). Our research group earlier performed blocking experiments to confirm the MC1-R specificity of these ^{68}Ga-labelled imaging probes, the previous findings of Nagy *et al.* had already strengthened the selective affinity of amide derivatives towards these receptors (Nagy et al., 2017). As we described in our previous studies, we performed blocking experiments in MC1-R expressing B16-F10 tumor-bearing mice with the co-injection of 15.6 ± 1.2 MBq of ^{44}Sc- or ^{68}Ga-labelled DOTA-NAPamide and 200 μg α-MSH - as blocking agent - in 100 μL saline. An hour postinjection, both the *in vivo* and *ex vivo* tracer distribution pattern was assessed. The significantly lower ($p < 0.01$) tracer accumulation of the blocked tumors verified the MC1-R binding specificity of the investigated radiolabelled NAPamide compounds (Nagy et al., 2017).

Given the marked tracer accretion of B16-F10 tumors, these novel MM specific molecular probes seem to be feasible in the detection of MC1-R positive malignancies. In a similar vein, Nagy *et al.* also substantiated the potential of both investigated ^{68}Ga and ^{44}Sc-labelled NAPamide derivatives in receptor positive melanoma identification (Nagy et al., 2017). However, they recorded more elevated SUV and T/M ratios in case of [^{44}Sc]Sc-DOTA-NAPamide 4 h post administration which could be explained by the physical characteristics and the more enhanced stability of ^{44}Sc (Nagy et al., 2017). Based on our results, the appropriate binding potential of [^{68}Ga]Ga-DOTA-NAPamide and [^{68}Ga]Ga-DOTA-HOLDamide to MC1-R made them ideal tracers for the authentication of receptor expressing B16-F10 experimental melanoma tumors in our experiment.

3.3. Impact of [^{213}Bi]Bi-DOTA-NAPamide and [^{213}Bi]Bi-DOTA-HOLDamide treatment on tumor growth and tumor volume

Body weight (expressed in grams) was normalized to the body weight measured on the 6th day (100%) post B16-F10 tumor cell implantation (relative body weight/RBW). Follow-up curves of RBW measurements - expressed as percentage - showed no significant change in any of the groups of the investigated animals ($p \leq 0.05$; as shown in Fig. 3**A**). The RBW figures of the control, untreated animal subclass were 100 ± 0.47, 103 ± 0.36, and 104 ± 0.88 measured on the 6th, 8th, and 10th days of the investigation; respectively. In the [^{213}Bi]Bi-DOTA-HOLDamide treated subcategory 100 ± 0.56, 101 ± 0.34, and 102 ± 0.95 were recorded on the given experimental days; respectively, while in the [^{213}Bi]Bi-DOTA-NAPamide cohort RBW was 100 ± 0.37 (6th day), 102 ± 0.41 (8th day) and 102 ± 0.69 (10th day). Lack of treatment-associated body weight loss might imply the safety of both

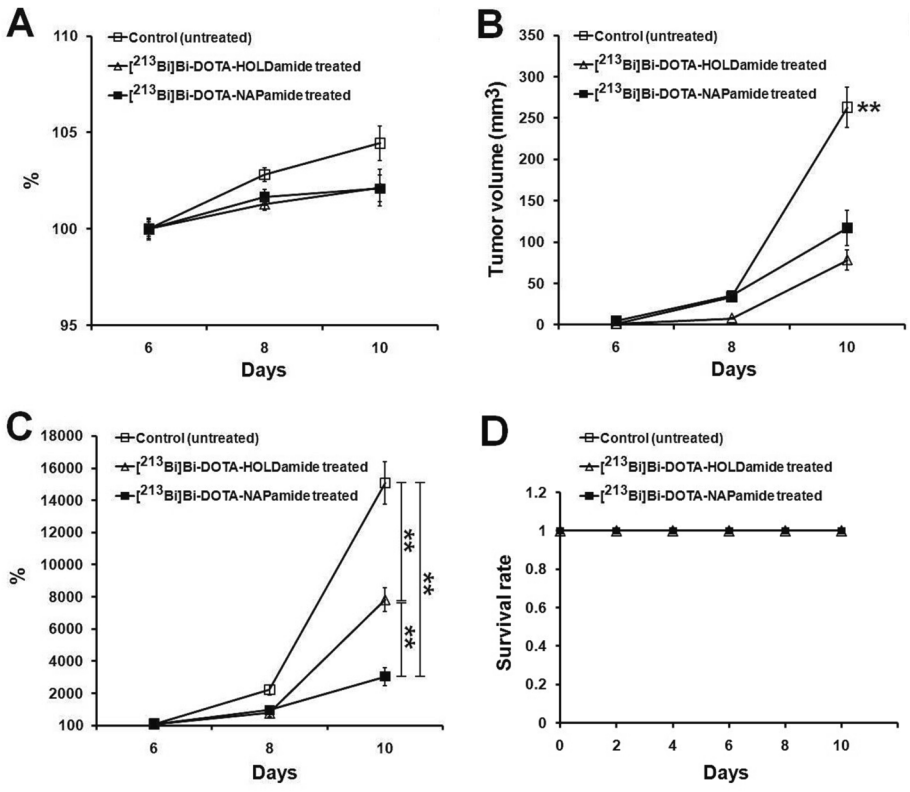

Fig. 3. Impact of [^{213}Bi]Bi-DOTA-NAPamide (n = 9) and [^{213}Bi]Bi-DOTA-HOLDamide (n = 6) treatment on body weight changes (A) and tumor growth (B and C). Data (gram) was normalized to the body weight measured on the 6th day (100%) post tumor cell injection (A). The treated tumor volume (mm^3) was compared to the volume of the control (untreated) tumors (B), and was normalized to the tumor volume registered on the 6th day (100%) post tumor cell transplantation (C). The survival rate of the animals until the day of euthanasia (D). Treatments began 6 days after B16-F10 tumor cell inoculation. Significance level: $p \leq 0.01$ (**), indicated in comparison with the treated B16-F10 tumors (B) and between the investigated groups (C).

investigated therapeutic agents. This may project the possible clinical applicability of these novel peptide-based anti-cancer drug-candidates. Nevertheless, further large-scale studies are required to uncover possible untoward side effects that may have an influence on their incorporation into clinical settings.

S.c. developing melanoma tumors of the control untreated group continuously expanded until the end of the experiment and reached a remarkable tumor volume of 262.83 ± 24.35 mm^3 by the 10th day. In the [^{213}Bi]Bi-DOTA-NAPamide treated subgroup a tumor size increase could also be observed with the subsequent mean tumor volumes: 4.83 ± 0.27 mm^3 on the 6th day, 35.33 ± 3.42 mm^3 on the 8th day, and 117.00 ± 21.07 mm^3 on the 10th day. Following the application of [^{213}Bi]Bi-DOTA-HOLDamide progressing tumor masses of 1.00 ± 0.14 mm^3, 7.75 ± 1.07 mm^3 and 78.25 ± 12.37 mm^3 could be registered on the 6th, 8th and 10th days; respectively. The treatments resulted in highly different follow-up curves. The continuity of tumor development could be tracked in Fig. 3**B.** Although no significant difference could be observed between the tumor expansion of the three animal groups on either the 6th or the 8th days ($p \leq 0.05$), the size of the tumors of the untreated mice measured on the 10th day was larger in comparison with either of the treated groups ($p \leq 0.01$). Based on this observation we may conclude that additional treatment regimens with enhanced anti-proliferative effects would induce further tumor growth reduction. Absence of difference between the tumor sizes of the treated subclasses might indicate the comparable therapeutic efficacy of the HOLDamide and NAPamide derivatives ($p \leq 0.05$).

Finally, the tumor bulks of the treated animals were normalized to those measured on the 6th day (100%) after the injection of the melanoma tumor cells. Follow-up curves of relative tumor masses (presented as percentage) are displayed in Fig. 3**C.** Constant tumor volume magnification was pinpointed in case of the untreated control animals with the following relative mean tumor volumes of 100 ± 8.32, 2220 ± 308.36, 15087 ± 1322.4 defined on the 6th, 8th, and 10th days; respectively. Similar tendency could be depicted in case of both subclasses of the treated mice, with 100 ± 4.67 (6th day), 775 ± 204.61 (8th day) and 7825 ± 721.36 (10th day) relative values for the radiolabelled HOLDamide administered cohort. Relative tumor bulk data of 100 ± 6.32, 956 ± 105.63 and 3050 ± 562.36 were recorded on the 6th, 8th and 10th days; respectively regarding the [^{213}Bi]Bi-DOTA-NAPamide treated cohort. Similarly to the previous findings, no statistically significant difference could be encountered between the relative tumor masses of the assessed groups on the 6th and 8th experimental time points *($p \leq 0.05$),* whereas compared to the treated classes, the relative dimensions of the untreated small animals appeared to be more sizeable on the 10th day *($p \leq 0.01$).* In contrast, a notable difference was remarked between the tumor volumes of the [^{213}Bi]Bi-DOTA-NAPamide and the [^{213}Bi]Bi-DOTA-HOLDamide administered groups measured on the 10th day *($p \leq 0.01$).* Histological analysis demonstrated that the presence of necrosis and apoptosis was more frequent in the treated animals compared to the untreated counterparts (Supplementary material **Fig. S5.**). Overall, the size of the neoplasms treated with [^{213}Bi]Bi-DOTA-NAPamide was the smallest. According to this finding [^{213}Bi]Bi-DOTA-NAPamide seems to be superior to the HOLDamide compound in terms of therapeutic efficacy, however, future research evaluating more tumor-related parameters are warranted to confirm our hypothesis. During the experimental period and after the three treatments no animal death was recorded. Fig. 3**D** represents the survival rate of the experimental mice until the day of the euthanasia.

The above remarked observations are of pivotal importance from clinical point of view, since the application of radiolabelled, receptor-selective MM treatment could potentially lead to the deceleration or even the prohibition of primary disease progression and metastases formation. Further, the integration of these novel theranostics into the existing clinical pathways may revolutionize cancer treatment leading to the establishment of tailor-made targeted anti-tumor therapy.

3.4. *Ex vivo* organ distribution studies

To assess the organ distribution of [^{213}Bi]Bi-DOTA-HOLDamide and [^{213}Bi]Bi-DOTA-NAPamide as well as to uncover the differences between their radioactivity pattern *ex vivo* studies were performed 30, - and 90 min following the *i.v.* injection of approximately 5 MBq of both MC1-R specific radiopharmaceuticals. After dissection, the accumulated radioactivities of the blood, liver, spleen, kidneys, intestine, stomach, muscle, lung and the *s.c.* growing B16-F10 tumors were measured by a high-performance gamma counter. *Ex vivo* data are displayed in Supplementary Material **Table S4**.

Using either [^{213}Bi]Bi-DOTA-HOLDamide or [^{213}Bi]Bi-DOTA-NAPamide the highest %ID/g values were confirmed in the kidneys at both investigated time points ([^{213}Bi]Bi-DOTA-HOLDamide: 15.18 ± 4.83 and 9.25 ± 0.06, [^{213}Bi]Bi-DOTA-NAPamide: 13.56 ± 2.98 and 6.65 ± 0.31; 30, - and 90 min postinjection; respectively) and in the urine ([^{213}Bi]Bi-DOTA-HOLDamide: 366.84 ± 186.67 and 52.44 ± 24.83, [^{213}Bi]Bi-DOTA-NAPamide: 556.39 ± 129.25 and 25.34 ± 8.24; 30, - and 90 min after tracer application; respectively). This prominent urinary radiopharmaceutical accumulation - in line with the *in vivo* PET/MRI data obtained with the ^{68}Ga-labelled amide derivatives - indicates renal elimination. Although, despite the high renal activity in the ^{213}Bi-treated animals, no signs of renal damage were shown by routine histological (hematoxylin/eosin) and immunohistochemical (cell cycle-related Phospho-Histone H3 histone (phH3), and apoptosis-related Caspase-3 labelling) analyses (supplementary material Histology section; **Fig. S6.**). As mentioned above, we observed more enhanced [^{68}Ga]Ga-DOTA-HOLDamide uptake in the kidneys compared with [^{68}Ga]Ga-DOTA-NAPamide accumulation. As for the ^{213}Bi-labelled compounds, we did not encounter any difference between the renal uptake of the two amide molecules. We hypothesize that the labelling procedures and the physicochemical properties of the radiometals may partially underly this observation. Further, the structural differences between the NAPamide and the HOLDamide derivatives may also explain the experienced difference between the urinary uptake pattern of the two tracers. Moreover, we also hypothesize the binding of the HOLDamide molecule to non-specific targets or unknown off-targets (receptors, other cell surface molecules). Albeit, future studies are required to fully uncover this result. In addition, the presence of the two radiotracers did not show any difference in the blood at either time points.

Applying any of the ^{213}Bi-appended tracers, the relatively low or moderate uptake of the thoracic and abdominal organs and tissues correlated well with the *in vivo* SUV_{mean} values of [^{68}Ga]Ga-DOTA-HOLDamide and [^{68}Ga]Ga-DOTA-NAPamide. Thirty minutes post-application, the liver, the lungs, the stomach and the muscle were depicted with [^{213}Bi]Bi-DOTA-HOLDamide %ID/g values of 1.55 ± 0.43, 2.48 ± 0.77, 1.29 ± 0.68 and 0.55 ± 0.13; respectively, while as for [^{213}Bi]Bi-DOTA-NAPamide accumulation the subsequent *ex vivo* data were registered: 1.97 ± 0.04, 2.24 ± 0.13, 1.10 ± 0.14, 0.81 ± 0.19 for the liver, the lungs, the stomach and the muscle; respectively. The 90-minute *ex vivo* data also showed slight accumulation. The *ex vivo* organ distribution pattern of ^{68}Ga and ^{44}Sc-labelled, DOTA-conjugated NAPamide - *represented in the kidneys (approximately %ID/g: 2.43–3.97) and in other organs and tissues published by Nagy et al.* - was comparable to that of ours (Nagy et al., 2017). Given the similar findings of other former investigations with ^{67}Ga and ^{111}In, the exchange of the radiometal had no effect on either renal excretion or the uptake of the peptide derivatives (Cheng et al., 2007a; Cheng et al., 2007b; Froidevaux et al., 2005).

As indicated in Fig. 4**.** - except for the liver, lungs and the B16-F10 tumor itself – the [^{213}Bi]Bi-DOTA-HOLDamide uptake of the investigated organs showed a considerable decrease *($p \leq 0.01$)* from 30 min until the termination of the study (90th minute). Apart from hepatic, lienal and tumorous accumulation; however, the selected organs exhibited remarkably lower [^{213}Bi]Bi-DOTA-NAPamide activity at the 90th minute compared to that of measured 30 min postinjection *($p \leq$*

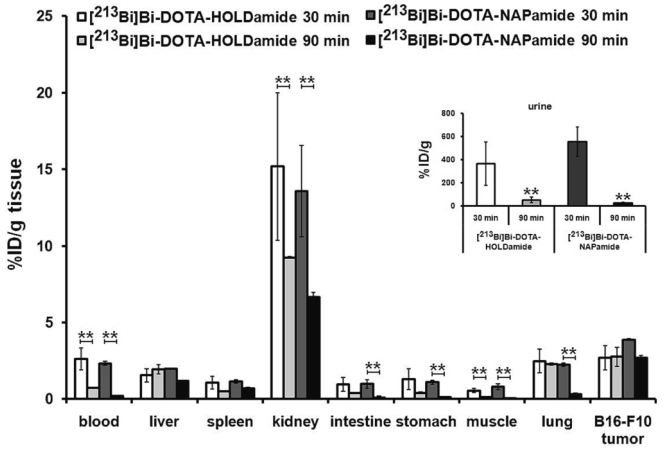

Fig. 4. *Ex vivo* biodistribution of [^{213}Bi]Bi-DOTA-HOLDamide and [^{213}Bi]Bi-DOTA-NAPamide in B16-F10 tumorous mice 30, - and 90 min postinjection of approximately 5 MBq of the MC1-R affine α-MSH-analogue radiopharmaceuticals. %ID/g tissue values are presented as mean ± SD. n = 5 mice/radiopharmaceutical/time point. Significance level between 30, - and 90 min for the corresponding radiopharmaceutical: $p \leq 0.01$ (**). MC1-R: Melanocortin-1 Receptor; α-MSH: Alpha-Melanocyte Stimulating Hormone; SD: standard deviation.

0.01) (as seen in Fig. 4.). Ninety minutes post administration of [^{213}Bi]Bi-DOTA-NAPamide the %ID/g values of the blood, kidney, intestine, stomach, muscle and lung were 0.19 ± 0.07, 6.65 ± 0.31, 0.09 ± 0.13, 0.12 ± 0.07, 0.02 ± 0.01, 0.32 ± 0.06; respectively.

Upon the assessment of the *s.c.* developing melanoma tumors, relatively enhanced %ID/g data were obtained in particular 90 min after [^{213}Bi]Bi-DOTA-NAPamide injection (%ID/g: 2.71 ± 0.15). Former literature findings also noted more elevated uptake of radiolabelled α-MSH analogues in preclinical MC1-R positive B16-F10 tumors in comparison with low receptor expressing A375 tumors (Breeman et al., 2011; Evans et al., 2020; Froidevaux et al., 2005). In addition, B16-F10 neoplasms were well identifiable with both [^{68}Ga]Ga-DOTA-NAPamide and [^{44}Sc]Sc-DOTA-NAPamide in a translational mouse model established by *Nagy and co-workers* (Nagy et al., 2017). Faint background activity together with relatively high uptake of the B16-F10 tumors result in satisfactory T/M ratios and image contrast, which purveys a clear added value in diagnostic applications (Breeman et al., 2011; Evans et al., 2020). As this phenomenon is of crucial importance in terms of reporting, it further outlines the future feasibility of ^{213}Bi-appended DOTA-NAPamide in image analyses and therapeutic follow-up as well. We could not reveal any meaningful difference during the comparison of the measurements of other organs (as presented in Fig. 4.).

Despite the above detailed promising results on the therapeutic efficacy of the radiolabelled peptide derivatives, however, some concerns regarding the use of ^{213}Bi must be addressed. First of all, the limited availability and the expenses of the mother isotope Actinum-225 (^{225}Ac) constitute a major drawback of the synthesis of ^{213}Bi (Dekempeneer et al., 2016). The short half-life of the radiometal ($T_{1/2}$ = 45.6 min) not only makes the transport of the isotope to remote facilities challenging, but also must be considered during the selection of the targeting vectors. Further owing to the short longevity of the radioisotope, applying [^{213}Bi]Bi-labelled probes for the treatment of easily achievable tumor cells is restricted (Majkowska-Pilip et al., 2020). Although several shortcomings may hamper the widespread application of ^{213}Bi, its usage circumvents the potential drawbacks of the therapeutic beta and Auger electron emitters. While beta rays exert considerable cytotoxic effects on healthy tissues, intracellular localization is needed for radionuclides with Auger electron emission to achieve relevant therapeutic effect (Marcu et al., 2018; Rosenkranz et al., 2020).

4. Limitations

There are some limitations of the present study that worth mentioning. The current research is lacking in some additional experiments that need to be executed to provide the complete performance evaluation of the investigated probes including but not limited to more detailed radiochemical investigations, *in vitro* affinity determination and blocking experiments. Based on our pioneering results, future studies with more advanced study design that addresses the evaluation of the therapeutic effect of the probes in tumor volumes of different sizes in a longer follow-up period are warranted. This would simultaneously ensure a more profound survival analysis as well. Further, instead of calliper measurements, more advanced imaging techniques such as CT or ultrasound should have been applied for the precise follow-up of tumor size change.

Although, the current research was primarily intended to be a proof-of-concept, raising the possibility that MC1-receptor-affine peptides labelled with alpha emitting ^{213}Bi may have a potential role in the targeted therapy of melanoma. Hence, we aimed at verifying whether either [^{213}Bi]Bi-DOTA-NAPamide or HOLDamide has any effects on tumor weight or tumor volume in order to determine which one is worthy of further *in vitro* and *in vivo* evaluations. Overall, our study was just a pioneering experiment that could lay the basis of detailed future studies conducted with these derivatives.

5. Conclusion

Overall, the *in vivo* diagnostic potential of [^{68}Ga]Ga-DOTA-NAPamide and [^{68}Ga]Ga-DOTA-HOLDamide to MC1-R overexpressing B16-F10 melanoma tumors could make them potential imaging PET probes for the identification of MC1-R positive MM. Our initial investigations may project the viability of alpha-emitting, MC1-R-targeting radiotheranostic agents in the targeted radionuclid therapy of both primary MM and related metastases. Nonetheless, future research with additional studies is warranted to fully strengthen the theranostic efficacy of the investigated ^{213}Bi-labelled peptide probes.

CRediT authorship contribution statement

Csaba Csikos: Visualization, Investigation, Conceptualization, Writing – original draft. **Zita Képes:** Methodology, Writing – review & editing. **Anikó Fekete:** Methodology. **Adrienn Vágner:** Investigation, Methodology, Visualization. **Gábor Nagy:** Investigation, Methodology, Visualization. **Barbara Gyuricza:** Investigation, Methodology, Visualization. **Viktória Arató:** Methodology. **Levente Kárpáti:** Investigation, Methodology, Visualization. **István Mándity:** Methodology, Writing – review & editing. **Frank Bruchertseifer:** Conceptualization. **Gábor Halmos:** Conceptualization, Supervision. **Dezső Szikra:** Conceptualization, Writing – review & editing. **György Trencsényi:** Writing – review & editing, Supervision.

Declaration of Competing Interest

The authors declare that they have no known competing financial interests or personal relationships that could have appeared to influence the work reported in this paper.

Data availability

Data will be made available on request.

Acknowledgements

This research work was conducted with the support of the National Academy of Scientist Education Program of the National Biomedical Foundation under the sponsorship of the Hungarian Ministry of Culture

and Innovation (Cs.Cs. and Gy.T.). The published work was supported by the Thematic Excellence Programme (TKP2020-NKA-04) of the Ministry for Innovation and Technology in Hungary. The work was also supported by the GINOP-2.3.2-15-2016-00043 (G.H.) grant co-financed by the European Union and the State of Hungary through the European Regional Development Fund, and by the Thematic Excellence Programme TKP2021-EGA-20 (Biotechnology) of the Ministry for Innovation and Technology in Hungary (G.H.).

Appendix A. Supplementary material

Supplementary data to this article can be found online at https://doi.org/10.1016/j.ijpharm.2023.123344.

References

Abbas, Rizvi, S.M., Sarkar, S., Goozee, G., Allen, B.J., 2000. Radioimmunoconjugates for targeted alpha therapy of malignant melanoma. Melanoma Res. 10, 281–289.

Ahenkorah, S., Cassells, I., Deroose, C.M., Cardinaels, T., Burgoyne, A.R., Bormans, G., Ooms, M., Cleeren, F., 2021. Bismuth-213 for Targeted Radionuclide Therapy: From Atom to Bedside. Pharmaceutics 13, 599. https://doi.org/10.3390/pharmaceutics13050599.

Allen, B.J., Rizvi, S.M., Tian, Z., 2001. Preclinical targeted alpha therapy for subcutaneous melanoma. Melanoma Res. 11, 175–182. https://doi.org/10.1097/00008390-200104000-00013.

Barca, C., Griessinger, C.M., Faust, A., Depke, D., Essler, M., Windhorst, A.D., Devoogdt, N., Brindle, K.M., Schäfers, M., Zinnhardt, B., Jacobs, A., H.,, 2021. Expanding Theranostic Radiopharmaceuticals for Tumor Diagnosis and Therapy. Pharmaceuticals (Basel) 15, 13. https://doi.org/10.3390/ph15010013.

Breeman, W.A., de Blois, E., Sze Chan, H., Konijnenberg, M., Kwekkeboom, D.J., Krenning, E.P., 2011. (68)Ga-labeled DOTA-peptides and (68)Ga-labeled radiopharmaceuticals for positron emission tomography: current status of research, clinical applications, and future perspectives. Semin. Nucl. Med. 41, 314–321. https://doi.org/10.1053/j.semnuclmed.2011.02.001.

Brzoska, T., Luger, T.A., Maaser, C., Abels, C., Böhm, M., 2008. Alpha-melanocyte-stimulating hormone and related tripeptides: biochemistry, antiinflammatory and protective effects in vitro and in vivo, and future perspectives for the treatment of immune-mediated inflammatory diseases. Endocr. Rev. 29, 581–602. https://doi.org/10.1210/er.2007-0027.

Castillo, Seoane, D., De Saint-Hubert, M., Ahenkorah, S., Vargas, C., Ooms, M., Struelens, L., Koole, M., 2022. Gamma counting protocols for the accurate quantification of 225Ac and 213Bi without the need for a secular equilibrium between parent and gamma-emitting daughter. EJNMMI Radiopharm. Chem. 7, 28. https://doi.org/10.1186/s41181-022-00174-z.

Cheng, Z., Chen, J., Miao, Y., Owen, N.K., Quinn, T.P., Jurisson, S.S., 2002. Modification of the structure of a metallopeptide: synthesis and biological evaluation of 111In-labeled DOTA-conjugated rhenium-cyclized alpha-MSH analogues. J. Med. Chem. 45, 3048–3056. https://doi.org/10.1021/jm010408m.

Cheng, Z., Xiong, Z., Subbarayan, M., Chen, X., Gambhir, S.S., 2007a. 64Cu-labeled alpha-melanocyte-stimulating hormone analog for microPET imaging of melanocortin 1 receptor expression. Bioconjug. Chem. 18, 765–772. https://doi.org/10.1021/bc060306g.

Cheng, Z., Zhang, L., Graves, E., Xiong, Z., Dandekar, M., Chen, X., Gambhir, S.S., 2007b. Small-animal PET of melanocortin 1 receptor expression using a 18F-labeled alpha-melanocyte-stimulating hormone analog. J. Nucl. Med. 48, 987–994. https://doi.org/10.2967/jnumed.107.039602.

Dekempeneer, Y., Keyaerts, M., Krasniqi, A., Puttemans, J., Muyldermans, S., Lahoutte, T., D'huyvetter, M., Devoogdt N, 2016. Targeted alpha therapy using short-lived alpha-particles and the promise of nanobodies as targeting vehicle. Expert Opin. Biol. Ther. 16, 1035–1047. https://doi.org/10.1080/14712598.2016.1185412.

Dekempeneer, Y., Caveliers, V., Ooms, M., Maertens, D., Gysemans, M., Lahoutte, T., Xavier, C., Lecocq, Q., Maes, K., Covens, P., Miller, B.W., Bruchertseifer, F., Morgenstern, A., Cardinaels, T., D'Huyvetter, M., 2020. Therapeutic Efficacy of 213Bi-labeled sdAbs in a Preclinical Model of Ovarian Cancer. Mol. Pharm. 17, 3553–3566. https://doi.org/10.1021/acs.molpharmaceut.0c00580.

Evans, B.J., King, A.T., Katsifis, A., Matesic, L., Jamie, J.F., 2020. Methods to Enhance the Metabolic Stability of Peptide-Based PET Radiopharmaceuticals. Molecules 25, 2314. https://doi.org/10.3390/molecules25102314.

Filippi, L., Chiaravalloti, A., Schillaci, O., Cianni, R., Bagni, O., 2020. Theranostic approaches in nuclear medicine: current status and future prospects. Expert Rev. Med. Devices 17, 331–343. https://doi.org/10.1080/17434440.2020.1741348.

Froidevaux, S., Calame-Christe, M., Schuhmacher, J., Tanner, H., Saffrich, R., Henze, M., Eberle, A.N., 2004. A gallium-labeled DOTA-alpha-melanocyte-stimulating hormone analog for PET imaging of melanoma metastases. J. Nucl. Med. 45, 116–123.

Froidevaux, S., Calame-Christe, M., Tanner, H., Eberle, A.N., 2005. Melanoma targeting with DOTA-alpha-melanocyte-stimulating hormone analogs: structural parameters affecting tumor uptake and kidney uptake. J. Nucl. Med. 46, 887–895.

Gladfelter, P., Darwish, N.H.E., Mousa, S.A., 2017. Current status and future direction in the management of malignant melanoma. Melanoma Res. 27, 403–410. https://doi.org/10.1097/cmr.0000000000000379.

Kálmán-Szabó, I., Képes, Z., Fekete, A., Vágner, A., Nagy, G., Szücs, D., Gyuricza, B., Arató, V., Varga, J., Kárpáti, L., Garai, I., Mándity, I., Bruchertseifer, F., Elek, J., Szikra, D., Trencsényi, G., 2023. In Vivo evaluation of newly synthesized 213Bi-conjugated alpha-melanocyte stimulating hormone (α-MSH) peptide analogues in melanocortin-1 receptor (MC1-R) positive experimental melanoma model. J. Pharm. Biomed. Anal. 229, 115374 https://doi.org/10.1016/j.jpba.2023.115374.

Kratochwil, C., Giesel, F.L., Bruchertseifer, F., Mier, W., Apostolidis, C., Boll, R., Murphy, K., Haberkorn, U., Morgenstern, A., 2014. ^{213}Bi-DOTATOC receptor-targeted alpha-radionuclide therapy induces remission in neuroendocrine tumours refractory to beta radiation: a first-in-human experience. Eur. J. Nucl. Med. Mol. Imaging. 41, 2106–2119. https://doi.org/10.1007/s00259-014-2857-9.

Majkowska-Pilip, A., Gawęda, W., Żelechowska-Matysiak, K., Wawrowicz, K., Bilewicz, A., 2020. Nanoparticles in Targeted Alpha Therapy. Nanomaterials (Basel). 10, 1366. https://doi.org/ 10.3390/nano10071366.

Mándity, I.M., Olasz, B., Ötvös, S.B., Fülöp, F., 2014. Continuous-flow solid-phase peptide synthesis: a revolutionary reduction of the amino acid excess. ChemSusChem 7, 3172–3176. https://doi.org/10.1002/cssc.201402436.

Mándity, I.M., Ötvös, S.B., Szőllősi, G., Fülöp, F., 2016. Harnessing the Versatility of Continuous-Flow Processes: Selective and Efficient Reactions. Chem. Rec. 16, 1018–1033. https://doi.org/10.1002/tcr.201500286.

Marcu, L., Bezak, E., Allen, B.J., 2018 Mar. Global comparison of targeted alpha vs targeted beta therapy for cancer: In vitro, in vivo and clinical trials. Crit. Rev. Oncol. Hematol. 123, 7–20. https://doi.org/10.1016/j.critrevonc.

Marin, J.F.G., Nunes, R.F., Coutinho, A.M., Zaniboni, E.C., Costa, L.B., Barbosa, F.G., Queiro, M.A., Cerri, G.G., Buchpiguel, C.A., 2020. Theranostics in nuclear medicine: emerging and re-emerging integrated imaging and therapies in the era of precision oncology. Radiographics 40, 1715–1740. https://doi.org/10.1148/rg.2020200021.

Morgenstern, A., Bruchertseifer, F., Apostolidis, C., 2012. Bismuth-213 and actinium-225 – generator performance and evolving therapeutic applications of two generator-derived alpha-emitting radioisotopes. Curr. Radiopharm. 5, 221–227. https://doi.org/10.2174/1874471011205030221.

Morgenstern, A., Apostolidis, C., Kratochwil, C., Sathekge, M., Krolicki, L., Bruchertseifer, F., 2018. An Overview of Targeted Alpha Therapy with 225Actinium and 213Bismuth. Curr. Radiopharm. 11, 200–208. https://doi.org/10.2174/1874471011666180502104524.

Nagy, G., Dénes, N., Kis, A., Szabó, J.P., Berényi, E., Garai, I., Bai, P., Hajdu, I., Szikra, D., Trencsényi, G., 2017. Preclinical evaluation of melanocortin-1 receptor (MC1-R) specific 68Ga- and 44Sc-labeled DOTA-NAPamide in melanoma imaging. Eur. J. Pharm. Sci. 106, 336–344. https://doi.org/10.1016/j.ejps.2017.06.026.

Norenberg, J.P., Krenning, B.J., Konings, I.R., Kusewitt, D.F., Nayak, T.K., Anderson, T. L., de Jong, M., Garmestani, K., Brechbiel, M.W., Kvols, L.K., 2006. 213Bi-[DOTA0, Tyr3]octreotide peptide receptor radionuclide therapy of pancreatic tumors in a preclinical animal model. Clin. Cancer Res. 12, 897–903. https://doi.org/10.1158/1078-0432.ccr-05-1264.

Poty, S., Francesconi, L.C., McDevitt, M.R., Morris, M.J., Lewis, J.S., 2018. α-Emitters for Radiotherapy: From Basic Radiochemistry to Clinical Studies-Part 2. J. Nucl. Med. 59, 1020–1027. https://doi.org/10.2967/jnumed.117.204651.

Rosenkranz, A.A., Slastnikova, T.A., Georgiev, G.P., Zalutsky, M.R., Sobolev, A.S., 2020. Delivery systems exploiting natural cell transport processes of macromolecules for intracellular targeting of Auger electron emitters. Nucl. Med. Biol. 80–81, 45–56. https://doi.org/10.1016/j.nucmedbio.2019.11.005.

Sadler, A.W.E., Hogan, L., Fraser, B., Rendina, L.M., 2022. Cutting edge rare earth radiometals: prospects for cancer theranostics. EJNMMI Radiopharm. Chem. 7, 21. https://doi.org/10.1186/s41181-022-00173-0.

Sgouros, G., Bodei, L., McDevitt, M.R., Nedrow, J.R., 2020. Radiopharmaceutical therapy in cancer: clinical advances and challenges. Nat. Rev. Drug Discov. 19, 589–608. https://doi.org/10.1038/s41573-020-0073-9.

Tafreshi, N.K., Tichacek, C.J., Pandya, D.N., Doligalski, M.L., Budzevich, M.M., Kil, H., Bhatt, N.B., Kock, N.D., Messina, J.L., Ruiz, E.E., Delva, N.C., Weaver, A., Gibbons, W.R., Boulware, D.C., Khushalani, N.I., El-Haddad, G., Triozzi, P.L., Moros, E.G., McLaughlin, M.L., Wadas, T.J., Morse, D.L., 2019. Melanocortin 1 Receptor-Targeted α-Particle Therapy for Metastatic Uveal Melanoma. J. Nucl. Med. 60, 1124–1133. https://doi.org/10.2967/jnumed.118.217240.

von Hacht, J.L., Erdmann, S., Niederstadt, L., Prasad, S., Wagener, A., Exner, S., Beindorff, N., Brenner, W., Grötzinger, C., 2019. Increasing molar activity by HPLC purification improves 68Ga-DOTA-NAPamide tumor accumulation in a B16/F1 melanoma xenograft model. PLoS One 14, e0217883.

Wild, D., Frischknecht, M., Zhang, H., Morgenstern, A., Bruchertseifer, F., Boisclair, J., Provencher-Bolliger, A., Reubi, J.C., Maecke, H.R., 2011. Alpha- versus beta-particle radiopeptide therapy in a human prostate cancer model (213Bi-DOTA-PESIN and 213Bi-AMBA versus 177Lu-DOTA-PESIN). Cancer Res. 71, 1009–1018. https://doi.org/10.1158/0008-5472.can-10-1186.